Journal of Power Sources 196 (2011) 6911–6914

Contents lists available at ScienceDirect

Journal of Power Sources

journal homepage: www.elsevier.com/locate/jpowsour

Short communication

Temperature dependent phosphorous oxynitride growth for all-solid-state batteries

S. Jacke*, J. Song, L. Dimesso, J. Brötz, D. Becker, W. Jaegermann

Technical University Darmstadt, Surface Science Department, Darmstadt, Germany

ARTICLE INFO

Article history:
Received 17 August 2010
Received in revised form 6 December 2010
Accepted 8 December 2010
Available online 21 December 2010

Keywords:
LiPON growth
Lithium-ion conductivity
Different structures
Doubly/triply bound nitrogen
Solid electrolyte
Impedance

ABSTRACT

LiPON (lithium-phosphorous-oxynitride), a solid state electrolyte for all-solid state Li ion batteries, was characterised in detail by XPS core level analysis. Different compositional structures were found for depositions at different sample temperatures. As known, the replacement of bridging oxygen by nitrogen plays an important role and the nitrogen XPS signal can be divided into two emission lines at different binding energies. These details have already been analysed in dependence on the deposition power and nitrogen pressure during deposition.

In this contribution we have investigated the LiPON deposition at different temperatures by XPS and impedance measurements. Different conductivity values could be linked to structural differences that were investigated by XPS core level analysis. Additionally, the activation energies were compared for the electrolytes obtained for depositions at different substrate temperatures.

1. Introduction

So far, liquid electrolyte batteries have dominated the rechargeable battery research field. Li-ion batteries using solid electrolytes exhibit the potential of miniaturisation for applications on chips, smart cards, etc. They also find applications in portable electronic devices.

One more important point is the safety aspect: solid electrolytes present advantages due to their thermal stability in contrast to liquid electrolytes [1,2]; avoidance of spillage [3] and often a large electrochemical window can be found [4], which avoids the iterative decomposition of the electrolyte [5]. This opens the possibility of using solid electrolytes also in large scale batteries as power sources for electrical vehicles or electrical tools. Solid electrolytes may also be used as thin layers in order to improve the conductivity.

The first solid electrolyte was introduced by Bates et al. [6] using LiPON (lithium-phosphorous-oxynitride). Since then, almost all of the all-solid state batteries used LiPON as the solid state electrolyte, apart from a few exceptions, e.g. the electrolyte presented by Yada et al. or Thangadurai et al. [7,8]; some other solid state electrolytes were chosen for testing, which did not have a large enough electrochemical window and therefore were not suitable for combination with either Li or the cathode material [4,9,10].

The LiPON electrolyte was used in different compositions by different groups or in combination with different materials [11–14]. So far, the best ionic conductivity of LiPON was found to be 3.3×10^{-6} S cm^{-1}, reported, for example, by Hamon et al. [15]. However, very different conductivity values have been reported ranging between 10^{-6} and 10^{-9} S cm^{-1} [16–18]. Therefore many research groups have started to investigate the influence of the fabrication parameters on the conductivity. In this context, the LiPON formation was investigated as a function of the sputter deposition parameters, i.e. the deposition power of the Rf sputtering [18–20] or the influence of the nitrogen pressure during sputtering in relation to the conductivity of the resulting LiPON film [11,17]. One focus was directed onto the nitrogen XPS signal and the bridging oxygen signal: the bridging oxygen signal decreased with increasing nitrogen content [19,21].

The nitrogen XPS signal is usually split into a contribution at higher and lower binding energy which is interpreted as doubly and triply coordinated nitrogen [6,20,21]. The expected partial molecular structure is shown in Fig. 1(a) and (b), taken from Hu et al. [22].

Du and Holzwarth [23] proposed that in a crystalline LiPON sample, the nitrogen may be bonded to two phosphate groups, but can be positioned close to a lithium site; this might also be detected as a triply coordinated nitrogen site.

Nonetheless, the signal at higher binding energies will be denoted here as N_t, at lower energies as N_d, for triply and doubly coordinated N, respectively. It has been claimed that the higher the N_t/N_d ratio, the higher will be the ionic conductivity of LiPON thin

* Corresponding author. Tel.: +49 6151 1669667; fax: +49 6151 166308.
E-mail address: sjacke@surface.tu-darmstadt.de (S. Jacke).

0378-7753/$ – see front matter © 2010 Elsevier B.V. All rights reserved.
doi:10.1016/j.jpowsour.2010.12.022

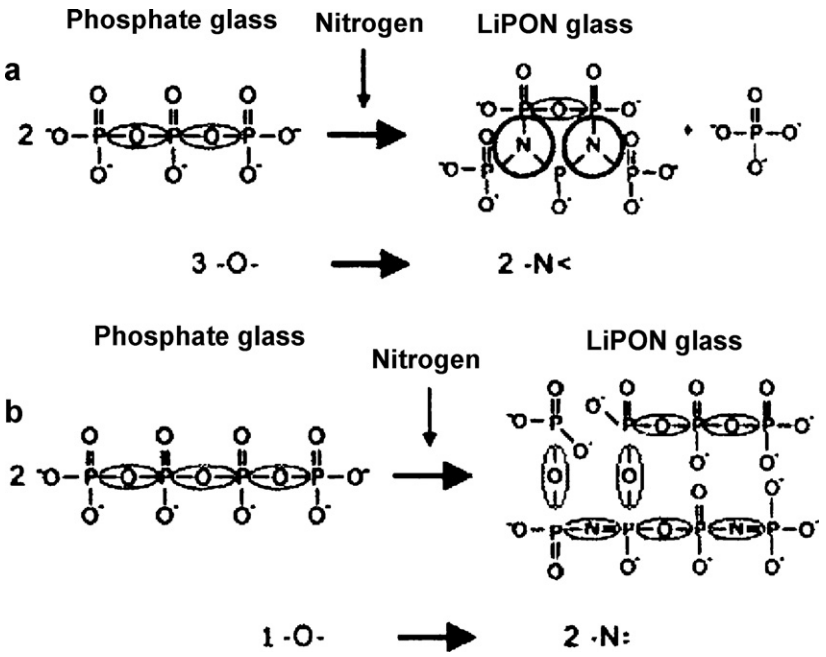

Fig. 1. Phosphate glass structure in the target before deposition and possible partial structures of the LiPON glass with nitrogen incorporation during deposition in nitrogen atmosphere, taken from Hu et al. [22].

films [22]. The ratio of these signals was found to be dependent on the power density during deposition, but the results are controversial. On one side Roh et al. [19] and Hamon et al. [15] observed an increase of the conductivity by decreasing the power density, on the other side Hu et al. [22] and Choi et al. [18] reported the opposite behaviour. Additionally, Iriyama et al. [24] investigated an influence of an annealing temperature of 473 K in air on the interface between $LiCoO_2$ and LiPON and found a decreased charge transfer resistance at the interface.

In this contribution we have investigated the influence of *in situ* heating during the LiPON deposition onto the conductivity, which could be linked to the structure observed in XPS. The LiPON deposition at room temperature was optimised achieving the highest conductivity for variable nitrogen pressure atmospheres during deposition and sputter power. For this reason, the conductivity achieved at room temperature lies close to the highest conductivities reported in the literature (as discussed above). This conductivity value increased when using LiPON deposition at higher temperatures, while leaving the other deposition parameters constant.

2. Experimental

The deposition of LiPON was carried out on an integrated UHV system allowing *in situ* transfer of samples from the deposition chamber to the XPS analysis chamber. The Rf sputter deposition took place under pure nitrogen atmosphere at a pressure of 8×10^{-3} mbar, using a Li_3PO_4 target with 2 in. diameter (provided by SCI Engineering). Deposition time was 6 h at 40 W with a pre-sputter time of 30 min. The base pressure of the chamber is 6×10^{-8} mbar. The temperature for LiPON deposition was without additional heating for the room temperature deposition, for the deposition at 200 °C and 300 °C, the sample substrate was heated to the respective temperature during the deposition. Thickness measurements were carried out on the cross section of the samples using electron microscopy (Philips XL 30 FEG, 30 kV).

The XPS system used was a Physical Electronics PHI-5700, with monochromatic Al K_α radiation with the energy of 1486.6 eV and a spectral resolution of 400 meV [25]. Survey scans were taken between 0 and 1400 eV, high resolution spectra were taken in the O1s, N1s, P2p and Li1s regions, no carbon was detected on the sample surface.

For a.c. impedance measurements a silicon/silicon-oxide/titanium-oxide substrate was used with sputtered platinum electrodes (in pure argon) that allowed 4 point measurements to confirm the homogeneity of the LiPON film; the equipment employed was a Princeton Applied Research, Model VPM 2 and a Zahner IM6. The measurements were carried out between 100 mHz and 100 kHz at room temperature. The resistance (R) was determined from the R(Re) data, where R(Im) goes through a local minimum [26], as indicated with an arrow in the Nyquist plots in Fig. 3 The resistivity was then calculated using the thickness measurements of the films. With the deposition masks used, a measurement area of 2 mm × 2 mm was obtained. The ionic conductivities were determined by using $\sigma = d/(R \times A)$, where d is the film thickness, A is the area of the metal contact, and R is the film resistance as provided by impedance measurements [26]. For the measurement of the activation energies, the a.c. impedance spectra were taken at different temperatures between room temperature and 55 °C in ca. 5 °C steps. The activation energies were determined graphically from Arrhenius plots, as reported by Bates et al. [6] and Wang et al. [21].

3. Results and discussion

The sputter parameters (such as power and nitrogen pressure) for the solid state electrolyte LiPON are optimised regarding the lithium ion conductivity. The structural differences were analysed for depositions at different sample temperatures. In this context, a dependence of the total amount of nitrogen and the amount of triply coordinated nitrogen on the sample temperature was found. The three different temperatures investigated were (1) LiPON deposition without additional *in situ* heating (room temperature), (2) at 200 °C and (3) at 300 °C. For each different temperature, a.c. impedance measurements were carried out. The impedance spectra are shown in Fig. 2 for LiPON in a Bode plot. In Fig. 3 the Nyquist plot is shown for these three deposition temperatures for comparison. An arrow shows the value of the half circle that was used

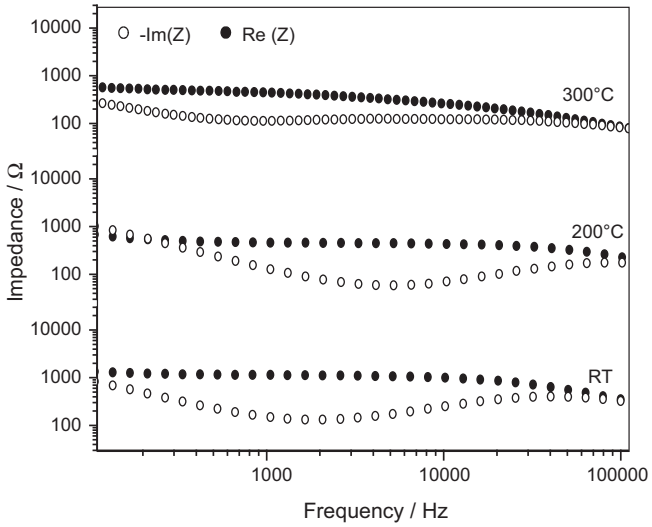

Fig. 2. Impedance measurements in a Bode plot in the frequency range between 1 and 10^6 Hz of LiPON deposited at room temperature (RT), at 200 °C and at 300 °C.

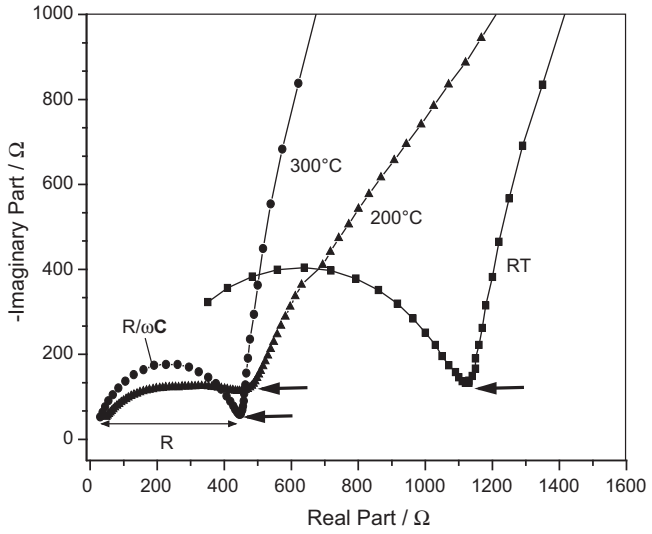

Fig. 3. Impedance measurements in a Nyquist plot in the frequency range between 1 and 10^6 Hz of LiPON deposited at room temperature (RT), at 200 °C and at 300 °C.

for further calculations. The calculated resistivities and respective activation energies are shown in Table 1. The resistivity decreases with increasing temperature during deposition, while the activation energy decreases slightly.

An XPS N1s investigation of the LiPON formation for different sample temperatures revealed an increasing nitrogen signal from deposition at room temperature until deposition at 300 °C. Part of it was an increase of the amount of the triply coordinated nitrogen, especially when comparing the deposition at 200 °C and 300 °C, as shown in Fig. 4. It is visible that the amount of triply coordinated nitrogen grew faster in the step between the deposition at 200 °C and 300 °C in proportion to the doubly coordinated nitrogen signal. The nitrogen

Table 1
Impedance measurements and activation energy.

Deposition temperature	σ ($\times 10^{-6}$ S cm^{-1})	act.E (eV)
(a) RT deposition	1.32 ± 0.04	0.53 ± 0.04
(b) Deposition at 200 °C	2.24 ± 0.04	0.48 ± 0.04
(c) Deposition at 300 °C	2.85 ± 0.04	0.47 ± 0.04

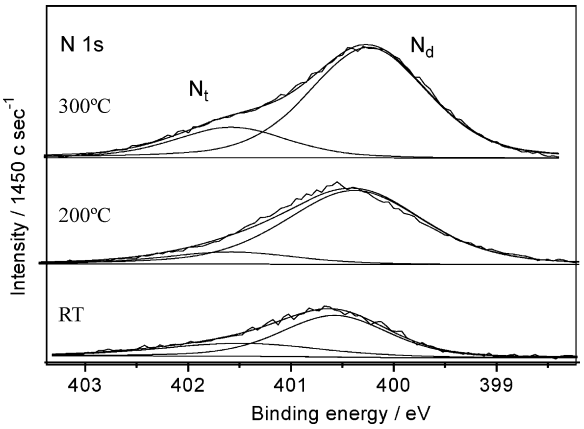

Fig. 4. XPS core level analysis of the amount of triply and doubly coordinated nitrogen at the deposition temperatures: room temperature (RT), 200 °C and 300 °C.

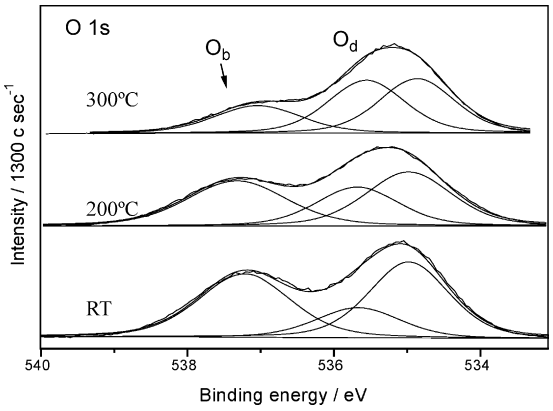

Fig. 5. XPS core level analysis of the qualitative ratios of bridging oxygen and an oxygen signal at higher binding energy at the deposition temperatures: room temperature (RT), 200 °C and 300 °C.

pressure during the sputter process was left constant. Structural analysis (X-ray diffraction) revealed that there was no change in the LiPON structure when deposited at higher temperatures.

A clear correlation of the nitrogen signal with the amount of bridging oxygen, Fig. 5, was found. We used the three component model for the fit of the oxygen XPS core level data [21]. The bridging oxygen decreases with the rising amount of nitrogen with higher deposition temperature, as shown in Fig. 4. Additionally, the amount of N_t has increased significantly for the deposition at 300 °C sample temperature – compared to 200 °C deposition, from ca. 15% to ca. 25% (calculated from the graphs, Fig. 4). The total amount of oxygen and nitrogen is shown in Table 2, as calculated from the XPS core level spectra and normalised to $P = 1$. The ratio of bridging to non-bridging oxygen was calculated according to the XPS core level spectra ratio between the peaks in the oxygen signal.

The growth of triply coordinated nitrogen makes the amount of bridging oxygen decrease faster, as discussed by Wang et al., who

Table 2
Amount of each LiPON component taken from XPS spectra, normalised to $P = 1$ and ratio of bridging to non-bridging oxygen.

Deposition temperature	Oxygen	Nitrogen ratio	O_b/O_{nb}
(a) RT deposition	2.4 ± 0.1	0.2 ± 0.1	0.40
(b) Deposition at 200 °C	2.3 ± 0.1	0.4 ± 0.1	0.37
(c) Deposition at 300 °C	2.1 ± 0.1	0.6 ± 0.1	0.23

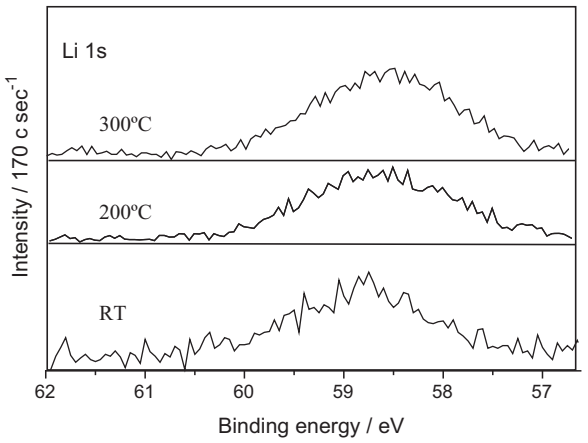

Fig. 6. XPS core level analysis of the lithium signal at the deposition temperatures: room temperature (RT), 200 °C and 300 °C.

suggested using a structural model proposed by Marchand et al. as one of the two possible models [21]. The faster decrease is visible in the comparison between the deposition at 200 °C and 300 °C: At a deposition at 300 °C, the amount of bridging oxygen was strongly reduced. At the same time, it is visible that the total amount of nitrogen has not increased strongly (Table 2), but the triply coordinated nitrogen has increased faster than the doubly coordinated nitrogen.

In contrast, the lithium signal increases slightly between the 200 °C and 300 °C substrate temperature deposition, as shown in Fig. 6.

We also found that a severe in depth nitridation of the target surface did not occur: when a reasonable pre-sputter time was used and a Li_3PO_4 (lithium phosphate) structure was sputtered, no nitridation was visible. This is in agreement with the results published by Choi et al. [18]. A significant change in the amount of nitrogen in the film composition because of a non-homogeneous target is therefore not expected for these sputter parameters.

The mechanism of the incorporation of nitrogen during the sputter process at different sample temperatures is assumed to be as follows: the bridging oxygen as it is present in the Li_3PO_4 structure is replaced by nitrogen, this may happen more effectively at higher temperature. The incorporation of nitrogen may already take place in the nitrogen environment that surrounds the sample, as proposed by Choi et al. [18]. They suggested that the nitrogen is directly incorporated into the structure from the plasma during its growth. According to Muñoz et al. [27], the cross linking density is therefore increased, which creates conduction paths with lower activation energy. Choi et al. [18] proposed that a lower deposition rate and therefore longer reaction time between the plasma and the thin film promotes the incorporation of nitrogen. We assume that the mechanism is comparable in this case, where a higher temperature may accelerate the reaction. The resulting LiPON films show higher nitrogen content when deposited at higher sample temperature and at the same time impedance measurements reveal a lower resistance.

We therefore assume that deposition at higher temperature is favourable for the LiPON Li^+-ion conductivity. However, interface formation with the electrodes and resulting properties will have to be investigated separately.

4. Conclusions

The dependence of the conductivity of the LiPON material on the temperature was demonstrated using three different temperatures for LiPON deposition: at room temperature, 200 °C and 300 °C. The LiPON films grown at different sample temperatures showed a decreasing amount of bridging oxygen with rising deposition temperature when investigated by core level XPS. The known correlation of an increase of the nitrogen content with the decrease of bridging oxygen could therefore be confirmed by these measurements. The films show increasing lithium ion conductivity with the increase of nitrogen content or increase of N_t.

These results, however, do not give any evidence about the charge transfer process of the cathode– or anode–LiPON interface, which has to be investigated separately. The difference of interface composition formed at different temperatures affects the structures at the LiPON/cathode or LiPON/anode heterogeneous interfaces and will be reported elsewhere.

Acknowledgements

The authors are grateful for the funding-DFG (SFB 595) and BMBF (LISA 03SF0327D 110005) and would like to thank Erich Golusda for his creative technical support. Many thanks to J. Schaffner and A. Fuchs for useful discussion and to M.I. Quintana for help with the manuscript.

References

[1] P.G. Balakrishnan, R. Ramesh, T.P. Kumar, J. Power Sources 155 (2006) 401–414.
[2] M. Armand, J.-M. Tarascon, Nature 451 (2008) 652–657.
[3] P. Yu, J.A. Ritter, R.E. White, B.N. Popov, J. Electrochem. Soc. 147 (2000) 1480–1485.
[4] J.B. Goodenough, J.B.Y. Kim, Chem. Mater. 22 (2010) 587–603.
[5] J.-M. Tarascon, M. Armand, Nature 414 (2001) 359–367.
[6] J.B. Bates, N.J. Dudney, G.R. Gruzalski, R.A. Zuhr, A. Choudry, C.F. Luck, J.D. Robertson, Solid State Ionics 53–56 (1992) 647–654.
[7] C. Yada, Y. Iriyama, T. Abe, K. Kikuchi, Z. Ogumi, Electrochem. Commun. 11 (2009) 413–416.
[8] V. Thangadurai, W. Weppner, J. Am. Ceram. Soc. 88 (2005) 411–418.
[9] P. Knauth, Solid State Ionics 180 (2009) 911–916.
[10] P. Birke, W.F. Chu, W. Weppner, Solid State Ionics 93 (1997) 1–15.
[11] S. Zhao, Z.F.Q. Qin, Thin Solid Films 415 (2002) 108–113.
[12] W.-J. Liu, J. Electrochem. Soc. 155 (2008) A8–A13.
[13] L. Baggetto, Adv. Funct. Mater. 18 (2008) 1057–1066.
[14] J.B. Bates, N.J. Dudney, B. Neudecker, A. Ueda, C.D. Evans, Solid State Ionics 135 (2000) 33–45.
[15] Y. Hamon, A. Douard, F. Sabary, C. Marcel, P. Vinatier, B. Pecquenard, A. Levasseur, Solid State Ionics 177 (2006) 257–261.
[16] J.B. Bates, N.J. Dudney, G.R. Gruzalski, R.A. Zuhr, J. Power Sources 43 (1993) 103–110.
[17] H.Y. Park, S.C. Nam, Y.C. Lim, K.G. Choi, K.C. Lee, G.B. Park, S.-R. Lee, H.P. Kim, S.B. Cho, J. Electroceram. Soc. 17 (2006) 1023–1030.
[18] C.H. Choi, W.I. Cho, B.W. Cho, H.S. Kim, Y.S. Yoon, Y.S. Tak, Electrochem. Solid-State Lett. 5 (2002) A14–A17.
[19] N.-S. Roh, S.-D. Lee, H.-S. Kwon, Scr. Mater. 42 (2000) 43–49.
[20] Y.G. Kim, H.N.G. Wadley, J. Vac. Sci. Technol. A 26 (2008) 174–183.
[21] B. Wang, B.S. Kwak, B.C. Sales, J.B. Bates, J. Non-Cryst. Solids 183 (1995) 297–306.
[22] Z. Hu, D. Li, K. Xie, Bull. Mater. Sci. 31 (2008) 681–686.
[23] Y.A. Du, N. Holzwarth, Phys. Rev. B 81 (2010) 184106.1–184106.15.
[24] Y. Iriyama, T. Kako, C. Yada, T. Abe, Z. Ogumi, Solid State Ionics 176 (2005) 2371–2376.
[25] A. Thissen, D. Ensling, M. Liberatore, Q.-H. Wu, F.J. Fernandez Madrigal, M.S. Bhuvaneswari, R. Hunger, W. Jaegermann, Ionics 15 (2009) 393–403.
[26] B. Kim, Y.S. Cho, J.-G. Lee, K.-H. Joo, K.-O. Jung, J. Oh, B. Park, H.-J. Sohn, T. Kang, J. Cho, Y.-S. Park, J.Y. Oh, J. Power Sources 109 (2009) 214–219.
[27] F. Muñoz, L. Pascual, A. Durán, R. Berjoan, R. Marchand, J. Non-Cryst. Solids 352 (2006) 3947–3952.